Original Article

Trends in Hearing
2015, Vol. 19: 1–12

DOI: 10.1177/2331216515569792
tia.sagepub.com

A Fast Method for Measuring Psychophysical Thresholds Across the Cochlear Implant Array

Julie A. Bierer[1], Steven M. Bierer[1], Heather A. Kreft[2], and Andrew J. Oxenham[2,3]

Abstract

A rapid threshold measurement procedure, based on Bekesy tracking, is proposed and evaluated for use with cochlear implants (CIs). Fifteen postlingually deafened adult CI users participated. Absolute thresholds for 200-ms trains of biphasic pulses were measured using the new tracking procedure and were compared with thresholds obtained with a traditional forced-choice adaptive procedure under both monopolar and quadrupolar stimulation. Virtual spectral sweeps across the electrode array were implemented in the tracking procedure via current steering, which divides the current between two adjacent electrodes and varies the proportion of current directed to each electrode. Overall, no systematic differences were found between threshold estimates with the new channel sweep procedure and estimates using the adaptive forced-choice procedure. Test–retest reliability for the thresholds from the sweep procedure was somewhat poorer than for thresholds from the forced-choice procedure. However, the new method was about 4 times faster for the same number of repetitions. Overall the reliability and speed of the new tracking procedure provides it with the potential to estimate thresholds in a clinical setting. Rapid methods for estimating thresholds could be of particular clinical importance in combination with focused stimulation techniques that result in larger threshold variations between electrodes.

Keywords

threshold, cochlear implant, psychophysics

Introduction

Cochlear implants (CIs) are neural prostheses for individuals who have severe or profound hearing loss. These devices consist of an array of electrodes that are inserted into the inner ear to stimulate the auditory nerve. The auditory nerve has a tonotopic organization, such that the frequency information carried by the nerve fibers changes systematically and in a topographic manner, with high frequencies represented by neurons that synapse near the basal end of the spiral cochlea and low frequencies represented by neurons that synapse closer to the apex. As such, different electrodes along the array are intended to activate specific populations of auditory nerve cells. By presenting each electrode with information from a limited frequency range, the prosthesis ideally recreates a tonotopic representation of sound in the implanted ear.

To adjust the dynamic range of the electrical current delivered to each electrode to the dynamic range of the acoustic input, audiologists have typically used psychophysical measures of the lowest detectable current level, called threshold, and the current level that is most comfortable for listening, called most comfortable level (MCL). Recently, however, some manufacturers have moved away from recommending threshold measurements, in part because the measurement procedure is considered too time consuming, and because thresholds are often quite uniform across the electrode array.

[1]Department of Speech and Hearing Sciences, University of Washington, Seattle, WA, USA
[2]Department of Otolaryngology, University of Minnesota, Minneapolis, MN, USA
[3]Department of Psychology, University of Minnesota, Minneapolis, MN, USA

Corresponding author:
Julie A. Bierer, Department of Speech and Hearing Sciences, University of Washington, 1417 NE 42nd St., Seattle, WA 98105, USA.
Email: jbierer@u.washington.edu

One reason for the relatively uniform absolute thresholds across the electrode array is the broad electrical field produced by the monopolar (MP) stimulation used in most commercially available implant systems. The broad stimulation fields produce uniform thresholds but also lead to poor tonotopic representation (e.g., Bierer & Middlebrooks, 2002). The poor tonotopic representation is thought to underlie at least some of the difficulties faced by CI users in understanding speech, especially in noisy environments (e.g., Friesen, Shannon, Baskent, & Wang, 2001; Litvak, Spahr, Saoji, & Fridman, 2007; Oxenham & Kreft, 2014).

In contrast to the single active electrode utilized for MP stimulation, focused stimulation can be achieved with CIs by manipulating the spatial arrangement of current delivery across the electrode array. Several such electrode configurations have been proposed over the past 20 years, including bipolar (BP), tripolar (TP), and partial tripolar (pTP), as well as the quadrupolar (QP) configuration employed in this study (Jolly, Spelman, & Clopton, 1996; Rodenhiser & Spelman, 1995). These configurations have been shown to produce narrower excitation patterns than MP stimulation, both physiologically (Bierer & Middlebrooks, 2002; Kral, Hartmann, Mortazavi, & Klinke, 1998; Snyder, Bierer, & Middlebrooks, 2004) and psychophysically (Bierer & Faulkner, 2010; Landsberger, Padilla, & Srinivasan, 2012; Long et al., 2014; Nelson, Donaldson, & Kreft, 2008). Although early studies failed to find clear perceptual benefits of focused stimulation (Pfingst, Franck, Xu, Bauer, & Zwolan, 2001; von Wallenberg et al., 1995; Zwolan, Kileny, Ashbaugh, & Telian, 1996), at least one recent study has shown improved understanding of speech in noise using pTP stimulation when compared with MP stimulation (Srinivasan, Padilla, Shannon, & Landsberger, 2013). Because focused stimulation produces narrower excitation patterns, it also commonly leads to more variable thresholds between electrodes. This is presumably because the density of surviving neurons and the distances between electrodes and those neurons are typically not uniform along the cochlear array (Bierer, 2010; Long et al., 2014; Teymouri et al., 2011). Therefore, if the use of focused stimulation techniques becomes more commonplace, threshold measurements may be reinstituted as a necessary step in fitting CIs in the clinic.

In acoustic hearing, fast methods for measuring thresholds and psychophysical tuning curves have been developed and validated for similar purposes. These methods are based on a variant of the Bekesy tracking technique (e.g., Zwicker, 1974), in which a listener adaptively adjusts the level of a tone, which glides slowly upward or downward in frequency, in order to maintain a threshold level of perception (Sek, Alcantara, Moore, Kluk, & Wicher, 2005; Sek & Moore, 2011). With these variants, the listener presses a button to indicate a tone is audible while the frequency of the tone is gliding. The level of the sound increases when the button is released and decreases when it is pressed. At face value, these methods appear difficult to implement in CIs because of the discrete nature of electrodes that represent sound frequency. However, technology in a subset of currently available CIs allows for quasi-continuous sweeps by using current steering—the stimulation of two neighboring electrodes simultaneously with a variable ratio of current between them, allowing for pitch percepts that are intermediate to those produced by the stimulation of the electrodes individually.

This study used virtual current sweeps to implement a procedure based on the Bekesy tracking method, thereby providing a rapid and clinically feasible measure of threshold across the electrode array. Thresholds obtained with this new method were compared with thresholds obtained using a traditional adaptive forced-choice procedure. The test–retest reliability of the two procedures was assessed, along with the respective test times. All procedures were performed with both a broad MP and focused QP electrode configuration.

Methods

Subjects

Fifteen postlingually deafened adults participated; all were implanted with the Advanced Bionics (Valencia, CA) HiRes90K CI. One subject was bilaterally implanted (S23, left ear and S36, right ear) to give a total of 16 ears tested. Details are shown in Table 1. Ten of the subjects were tested at the University of Washington in Seattle (subject identifiers with an "S") while the remaining five subjects were tested at the University of Minnesota in Minneapolis (subject identifiers with a "D"). The respective Human Subjects Review Boards approved all procedures, and all subjects provided written informed consent.

Stimuli

Biphasic, charge-balanced, cathodic-phase-first pulse trains were used. Phase durations were 97 μs and the pulse rate was 997.9 pulses per second. Each pulse train was 200.4 ms in duration and was presented either in MP or QP configuration (see Figure 1). All stimuli were presented and controlled using research hardware and software ("BEDCS") provided by the Advanced Bionics Corporation (version 1.18). Programs were written using the MATLAB programming environment, which controlled low-level BEDCS routines. Identical software and hardware were used at both testing sites (Minneapolis and Seattle).

Table 1. Subject Demographics.

Subject code	Gender	Age at start of experiment (Years)	CI use prior to experiment (Years)	Etiology	Duration bilateral severe-profound hearing loss prior to implant (Years)
D24	M	64.3	6.9	Unknown progressive	27
D26	F	55.0	5.5	Unknown	11
D28	F	65.6	11.6	Familial progressive SNHL	7
D33	M	74.7	1.3	Noise exposure; Trauma	<1
D38	F	32.6	1.3	Sudden SNHL	<1
S22	F	73.6	6.9	Unknown progressive	11.7
S23	M	69.0	7.0	Unknown progressive, sudden loss 10 years ago	7.9
S28	F	74.7	5.0	Autoimmune disease	18.7
S29	M	82.0	5.0	Unknown progressive	34.0
S30	F	49.0	10.0	Unknown progressive	16.0
S36[a]	M	69.1	4.5	Unknown progressive, sudden loss 8 years ago	3.5
S38	M	48.8	3.6	Otosclerosis	18.3
S40	M	51.7	1.3	Enlarged vestibular aqueduct	46.4
S41	M	48.6	5.6	Maternal rubella	1.2
S42	M	63.8	12.6	Sudden loss	33.5
S43	M	68.4	0.6	Unknown progressive	17.9

[a]Indicates the second ear of S23.

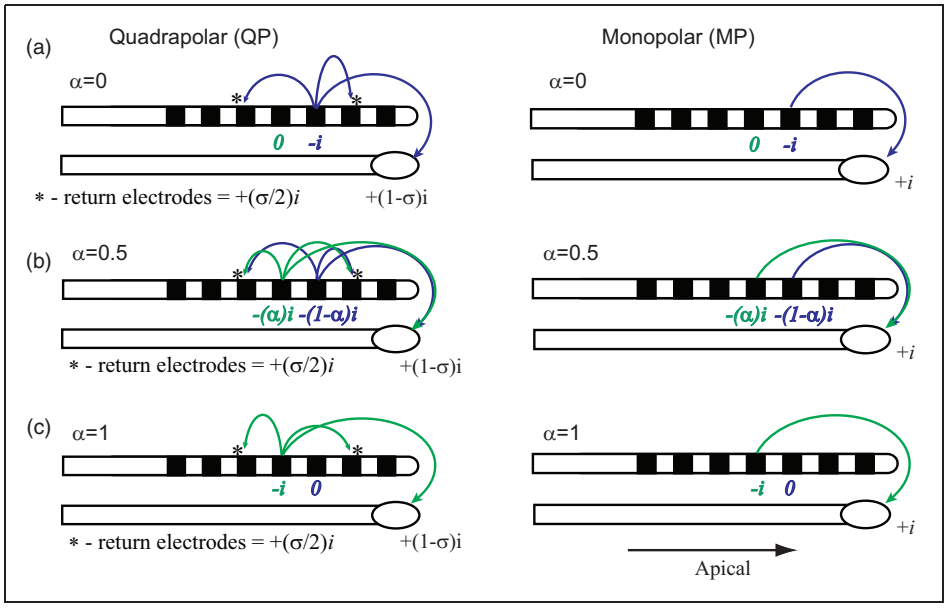

Figure 1. Schematic of steered QP (left) and MP (right) electrode configurations. QP consists of four adjacent electrodes; two active electrodes and two flanking return electrodes that share a fraction of the return current. The remaining current is delivered to an extracochlear ground electrode. Alpha represents the ratio of current for the two active electrodes. An alpha of 0 (a) indicates all stimulating current is delivered to the more apical electrode (panel a), while an alpha of 1 (c) indicates all current is directed to the basal electrode (panel c). Alpha equal to .5 (b) indicates half of the stimulating current is applied to each of the two active electrodes (panel b). In the MP configurations (right), all of the return current is delivered to the extracochlear ground electrode. Alpha nomenclature is the same for both configurations, and electrodes more apical are to the right.

The stimulation procedures for current focusing and steering with the QP configuration are illustrated in Figure 1. The QP configuration consists of two active electrodes and two adjacent flanking electrodes. With full QP, two flanking electrodes carry all of the return current evenly, which theoretically produces the most restricted current spread. With partial QP (left column of Figure 1), a fraction of return current, sigma (σ), is delivered to the flanking electrodes, and the remainder is delivered to an extracochlear ground. The broadest stimulation, corresponding to the MP configuration (right column), is achieved when all of the return current flows to the distant ground ($\sigma = 0$). In this experiment, the value of σ was fixed at .8 for one subject (D24) and at .9 for all other subjects. A σ value of .9 was selected because it allowed the measurement of suprathreshold stimulation while maintaining current levels lower than the voltage compliance limits of the device. For subject D24 a smaller σ value of .8 was necessary to remain below compliance limits.

The illustrations from top to bottom show the effects of changing the steering coefficient, alpha (α). At the top (panel a), all current is delivered through the more apical of the two active electrodes ($\alpha = 0$); in the middle (panel b), current is distributed equally ($\alpha = .5$); and at the bottom (panel c), all current is steered through the most basal active electrode ($\alpha = 1$). A particular set of electrodes and steering parameter defines a *channel*. Whether stimulated with a broad or focused electrode configuration, it is presumed that every channel produces a different spatial pattern of current in the cochlea.

Procedures

Sweep thresholds. Analogous to an upward acoustic frequency sweep, pulse trains were presented at regular time intervals while the alpha value was increased from 0 to 1 in .1 steps beginning with the most apical set of QP electrodes. Each 200.4 ms pulse train was followed by a 300 ms silent interval, for a repetition period of about 500 ms. The value of α was incremented every 1,000 ms, such that the same electrode and α combination occurred twice in succession during the sweep. This process was repeated without interruption for the next, more basal set of electrodes until all available sets were tested (active electrodes 2–15), resulting in a single *forward sweep*. At the beginning of the sweep, the signal was presented at a level of at least 3 dB below MCL. During the sweep, the listener was directed to hold the spacebar of a computer keyboard down when the signal was audible, causing the current level to decrease, and to release the spacebar when it became inaudible, causing the current level to increase. The current step size was 1 dB. The combination of an alpha value of .1 and a tracking step size of 1 dB was considered a good compromise between accuracy and duration, based on pilot data. A similar *reverse sweep* was obtained in the same manner but starting with the most basal set of QP electrodes and ending with the most apical. Current levels from one forward and one reverse sweep constituted a complete *run*, and two such runs were obtained for each subject. Subjects were often provided with a brief practice run that included only two or three electrodes. After this brief exposure, subjects were generally able to complete the task, although some noted that the task seemed difficult.

An example of a forward sweep for one subject is shown in Figure 2A. The graph depicts a portion of the data sequence beginning 40 s from the start of the sweep and encompassing active electrode pair 5/6, $\alpha = .5$, to electrode pair 6/7, $\alpha = .5$. Note that each electrode and α combination, or channel, is represented twice, because during a sweep each stimulus is repeated before proceeding to the next set of parameters.

Final threshold estimates for a run were obtained by a weighted averaging of consecutive current levels along the forward and reverse sweeps. This procedure is illustrated in Figure 2B, based on the same forward sweep as Figure 2A in addition to the complementary reverse sweep. First, a channel number was assigned to each stimulus by adding the alpha fraction to the number of the apical active electrode. In Figure 2, for example, a stimulus with active electrodes 5/6 and α parameter .8 is assigned a channel number of 5.8. The forward and reverse data points were then assigned to the appropriate location along the ordinate channel axis, as depicted by the blue and red points in Figure 2B. Note that "nonsteered" channels occurring at integer channel numbers (e.g., 6.0 in Figure 2B) have twice the number of data points as other channels; this is because these channels are created from two different sets of electrodes, one set with $\alpha = 1$ and a more basal set with $\alpha = 0$, such that the same electrode carries all of the active current for both channels (Electrode 6 in this example). Next, the data points corresponding to the individual channels were averaged together to produce a sequence of intermediate threshold estimates (not shown). Finally, a weighted average was calculated using a 5-point hamming window of length $\pm.2$ centered on the current value of α; the five channel weights, from apex to base, were .083, .25, .33, .25, and .083. The window length of $\pm.2$ was selected because it better matched the thresholds estimated with the standard procedure than a window length of $\pm.1$. In Figure 2B, the extent of the averaging window is indicated by the horizontal and dotted lines, and the resulting threshold estimate for channel 6.0 is shown by a black triangle. Averaging in this manner reduces the effect of hysteresis observed in unidirectional sweeps (Sek et al., 2005). Thresholds were calculated in this manner for every nonsteered integer-numbered channel, for direct comparison

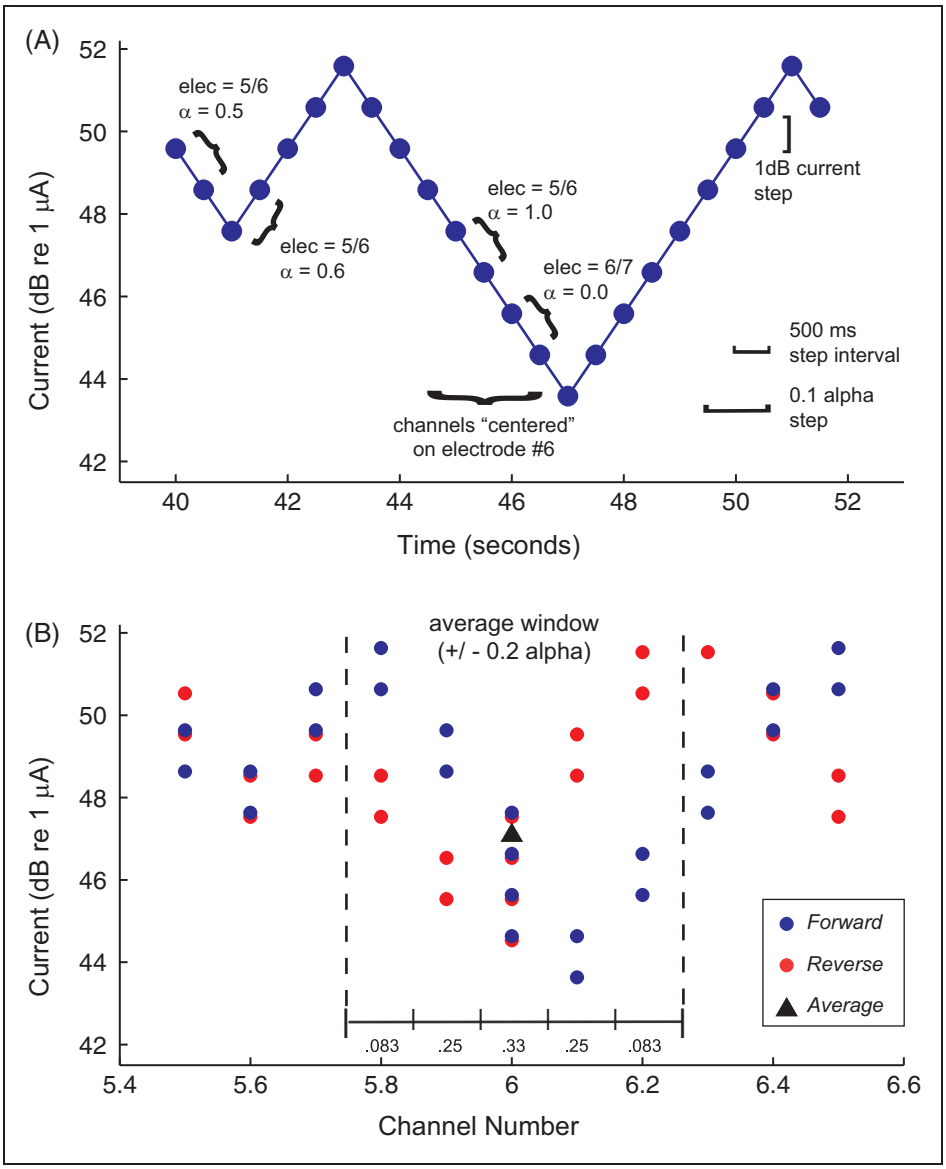

Figure 2. A sample of sweep data over time (A) and across channel numbers (B) for S29. (A) Stimulus level and active electrode number during a portion of a forward sweep. The *x*-axis is time in seconds and the *y*-axis is stimulus level in dB re 1 μA. The active electrodes and alpha values are indicated by each pair of symbols. (B) Stimulus level as a function of active channel number for a forward (blue) and reverse (red) sweep. The *x*-axis is channel number and the *y*-axis is stimulus level in dB re 1 μA. The gray bar centered at Channel 6 indicates the range of data used for the average threshold estimate (black triangle). The corresponding numbers indicate the weights applied to the data for each channel.

to thresholds estimated using the adaptive forced-choice method, described below.

Adaptive forced-choice thresholds

Clinically, when audiologists measure threshold behaviorally with CI listeners, a procedure is used that is similar to how pure-tone thresholds are measured for an audiogram, except that the listener is sometimes asked to count the beeps. Because the clinical procedures are not standardized across devices, a more scientific and precise procedure was selected for comparison to the sweep method described here. For each subject, detection thresholds were measured using a two-down, one-up, two-interval two-alternative forced-choice (2AFC) procedure converging on the 70.7% correct point of the psychometric function (Levitt, 1971). Each run began with the stimulus level at least 3 dB below MCL, and the level was initially increased or decreased by 2 dB depending on the listener's responses. After the first two reversals, the step size was decreased to .5 dB, where it remained for the final four reversals. The average stimulus level at

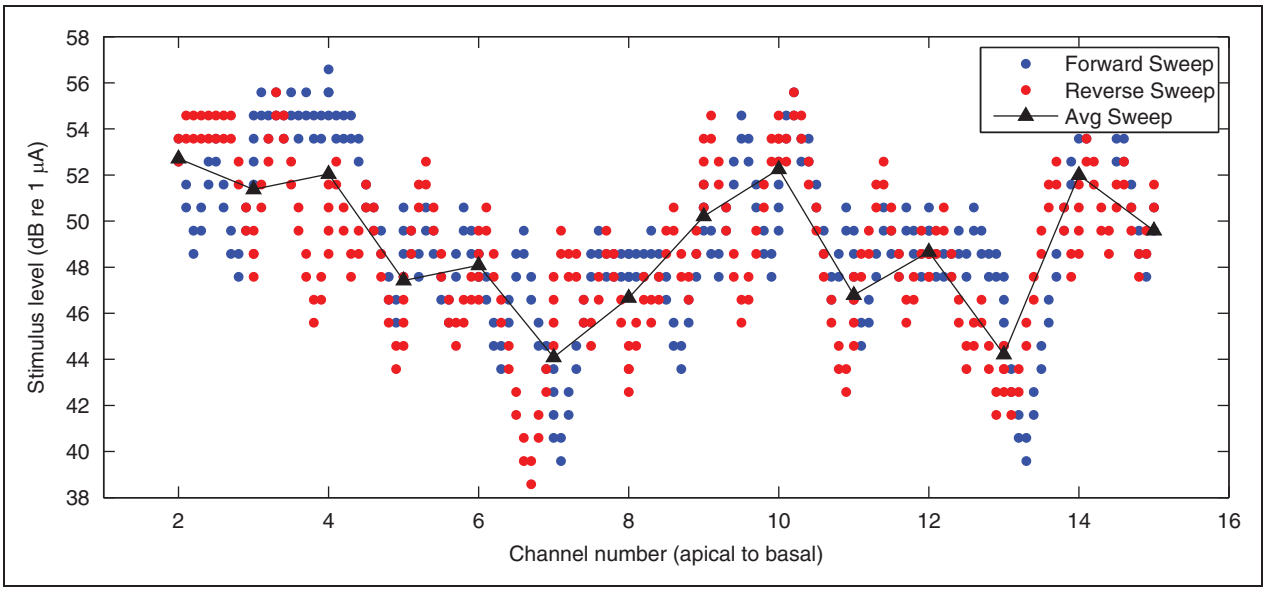

Figure 3. A full example of one forward (blue) and one reverse (red) sweep for S29. The *x*-axis is channel number and the *y*-axis is stimulus level in dB re 1 μA. The black triangles represent the average threshold estimate for each of the cardinal channel numbers.

the last four reversals was defined as threshold for that run. A final threshold was obtained as the average over four runs, with a fifth added if the standard deviation for the last four reversals was greater than 1.5 dB. Thresholds were measured for all available electrodes from 3 to 15 using the non-steered $\alpha = 1.0$, and for Electrode 2 using an alpha of 0. The same MP and QP configurations were used as for the sweep thresholds. The measurement order for electrode and stimulation method (2AFC and channel sweep) was randomized across repetitions and subjects.

Results

Figure 3 shows an example of one forward (blue) and one reverse (red) sweep, with current level plotted as a function of channel number from apex to base for subject S29. Black triangles depict the final threshold estimates of the run for each electrode-centered channel, following the weighted averaging procedure.

Comparison of Threshold Measures

Thresholds obtained with the traditional two-interval forced-choice (open symbols) and the channel sweep procedures (filled symbols) are shown for all individual subjects in Figure 4. The average thresholds for the QP (triangles) and MP configurations (circles) are plotted, along with the standard deviations estimated from the repeated measures (with $N = 2$ in the case of the sweep, and $N = 4$ or 5 in the case of the forced-choice procedure). Consistent with previous findings, thresholds in the more focused QP stimulation mode are higher and more variable than thresholds in the MP mode (Bierer, 2007; Long et al., 2014; Pfingst, Xu, & Thompson, 2004). Overall, the channel-to-channel threshold patterns of the two procedures match quite closely. The similarity of threshold estimates between the two procedures can also be observed in the mean data, shown in Figure 5. The scatter plot in Figure 6 compares thresholds from the individual subjects obtained using the two different procedures. Any systematic bias of the sweep procedure, relative to the forced-choice procedure, would be reflected in a tendency for the data points to fall predominantly above or below the major diagonal. No such bias is discernable from the plot. To investigate the possibility of systematic biases more rigorously, a within-subjects repeated-measures analyses of variance (ANOVAs) was carried out with threshold as the dependent variable and electrode number, stimulation mode (MP or QP), and procedure (sweep or forced-choice) as within-subjects factors. (All reported ANOVA results include a Huynh–Feldt correction for lack of sphericity where applicable.) The ANOVA revealed a significant main effect of stimulation mode ($F(1, 14) = 210.75$, $p < .001$), but no main effect of either electrode number or procedure. However, there were significant interactions between procedure and stimulation mode ($F(1, 14) = 11.07$, $p = .005$), as well as procedure and electrode number ($F(8.4, 118) = 5.001$, $p < .001$). The interaction between procedure and stimulation mode may reflect the trend apparent in Figure 5 for thresholds to be lower in the sweep than in the forced-choice procedure in the MP but not the QP mode. The interaction between procedure

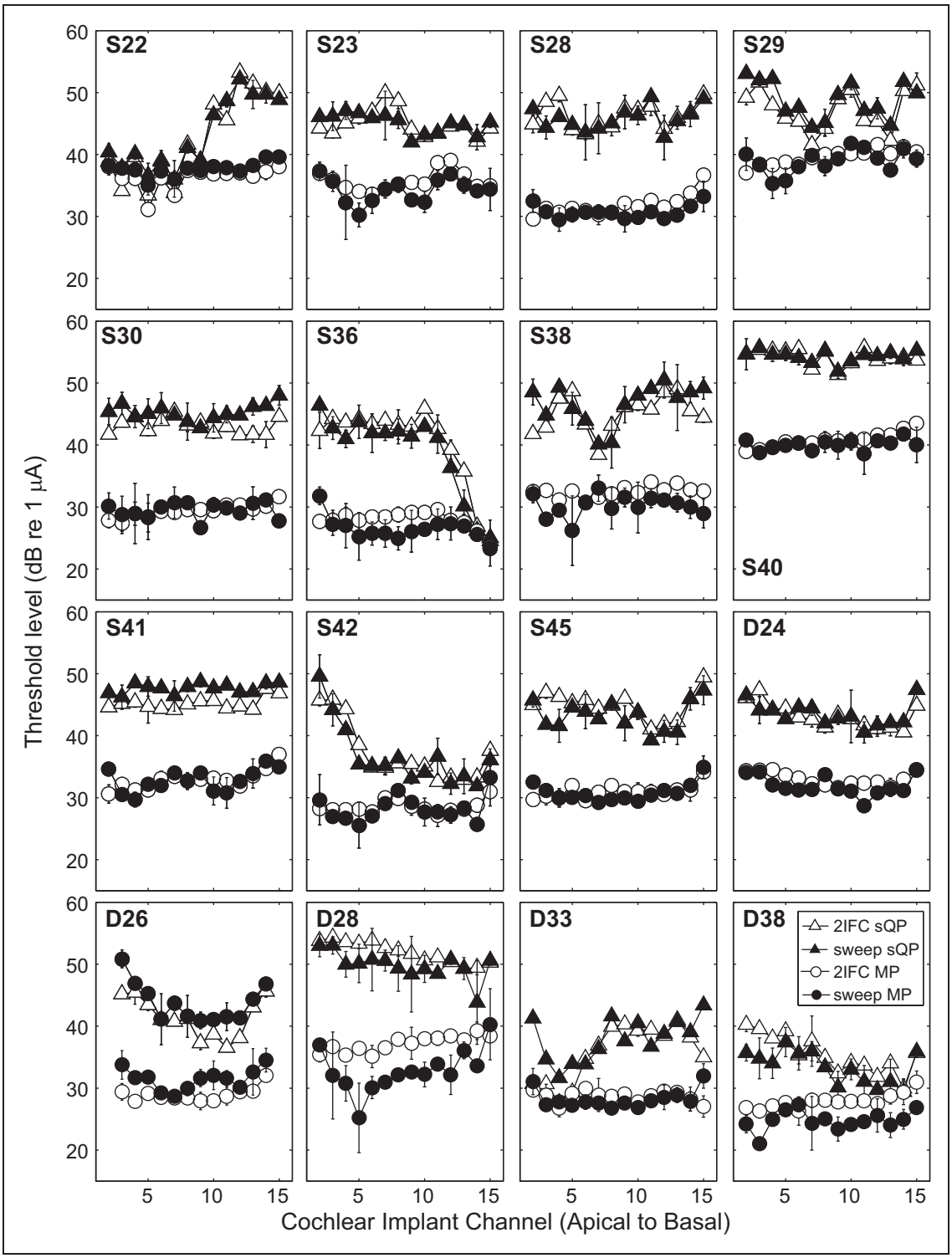

Figure 4. Detection thresholds measured with 2IFC methods (open) and sweep methods (filled) for all subjects individually. Thresholds for QP are indicated by triangles and MP by circles. Error bars represent ±1 standard deviation and are shown when they exceed the symbol size. The *y*-axis is stimulus current (dB re: 1 μA) and the *x*-axis is CI channel from apical to basal.

and electrode number is more difficult to interpret and may reflect the apparently different patterns observed at different electrode sites (e.g., sweep thresholds tend to be higher than forced-choice thresholds on Electrode 2, whereas the opposite is true for Electrode 9). Nevertheless, the relatively small (~1 dB) difference, along with a lack of a main effect of procedure, is consistent with the hypothesis that the sweep procedure does not introduce any systematic biases, relative to the thresholds obtained in the more standard adaptive forced-choice procedure.

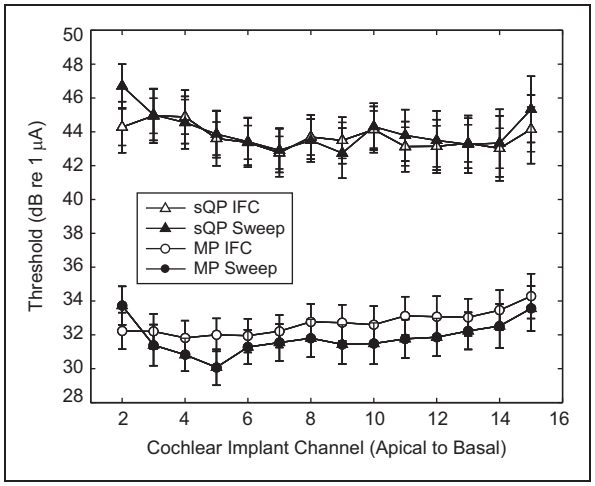

Figure 5. Detection thresholds averaged across all subjects as a function of electrode number for each stimulation mode and procedure. Error bars represent ±1 standard error of the mean. The *y*-axis is stimulus current (dB re: 1 μA) and the *x*-axis is CI channel from apical to basal.

Reliability of Threshold Measures

At least four estimates of threshold in the adaptive forced-choice procedure were made in order to provide a "gold-standard," with which to compare the new channel sweep threshold estimates, as described earlier. However, to assess the test–retest reliability of the two procedures, an equal number of runs were compared. As only two runs were collected in each subject for the channel sweep procedure (each consisting of one forward and one reverse sweep), only the first two of the adaptive forced-choice runs were included in this assessment. The comparisons between the first and second threshold estimates are shown as scatter plots in Figure 7, with the adaptive forced-choice and channel sweep procedures displayed in the top and bottom rows, respectively, and the MP and QP data in the left and right panels, respectively. In all panels, the first and second run threshold estimates qualitatively appear similar, with no apparent upward or downward biases. Test–retest reliability was evaluated quantitatively by subjecting the squared difference between the two estimates to a repeated-measures ANOVA, with electrode number, stimulation mode (MP or QP), and procedure as factors. The analysis revealed a significant main effect of procedure ($F(1, 12) = 11.36$, $p = .006$, partial $\eta^2 = .486$), as well as a marginally significant three-way interaction between stimulation mode, procedure and electrode number ($F(4.8, 57.3) = 2.63$, $p = .035$, partial $\eta^2 = .179$). The main effect of procedure is reflected in the square root of the mean squared (rms)

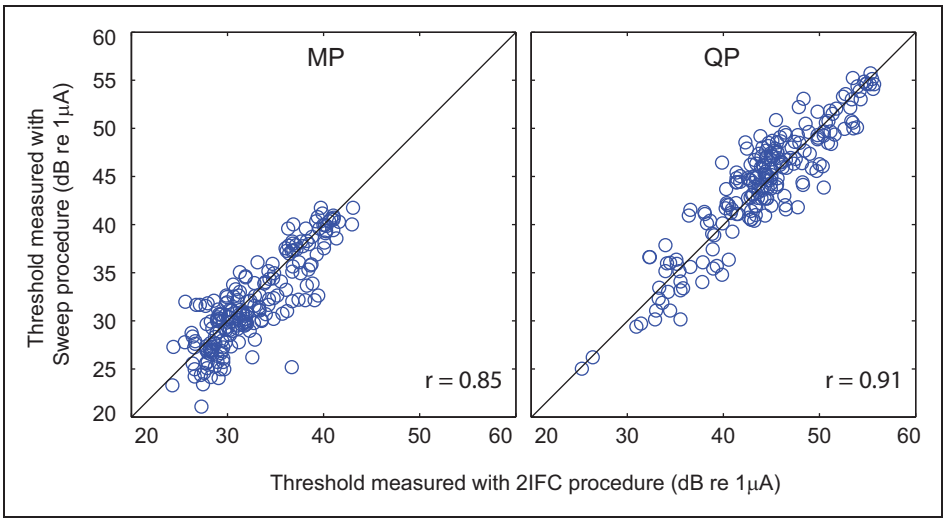

Figure 6. Comparison of thresholds estimated with 2IFC and sweep methods across all subjects. Each panel plots thresholds estimated by sweep method (*y*-axis) as a function of 2IFC method (*x*-axis) for the MP configuration data (left) and QP data (right). *R* values are based on Pearson's correlation analysis and were significant with a $p < .001$.

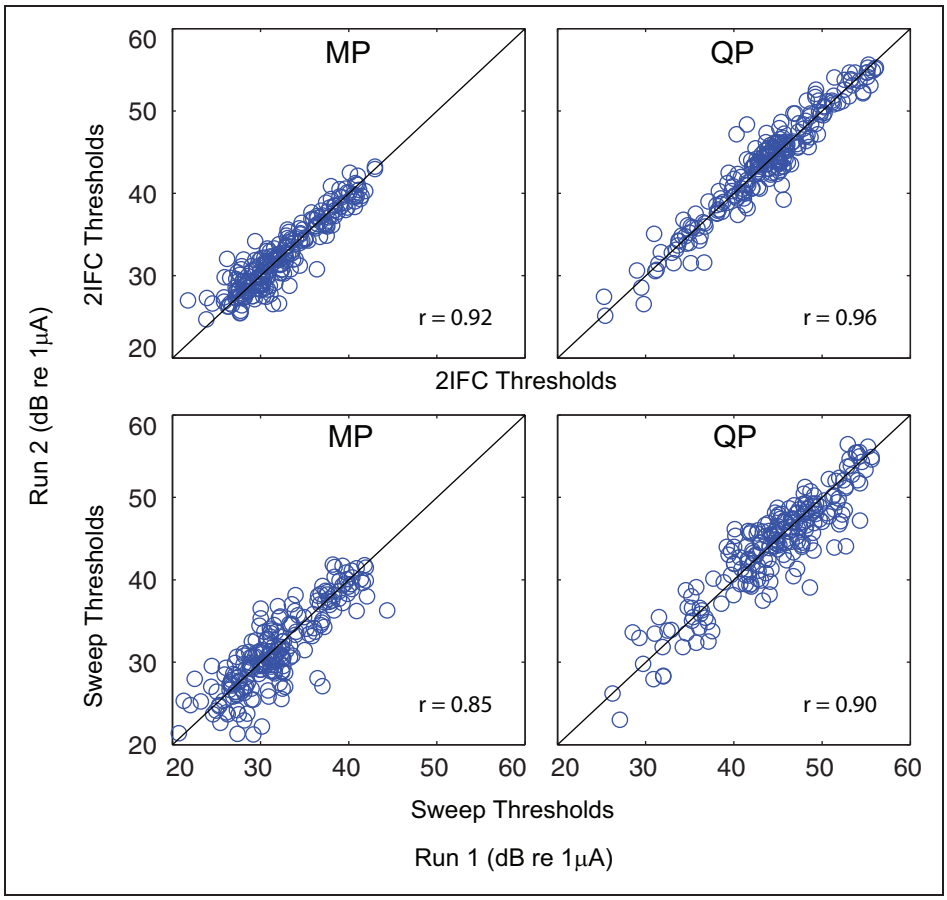

Figure 7. Test–retest reliability for 2IFC (top panels) and sweep (bottom panels) threshold estimates. Threshold estimates from the last two or three runs of the 2IFC procedure (*y*-axis) are plotted as a function of the first two 2IFC estimates (*x*-axis) for MP (top left) and QP (top right). Threshold estimates from the second forward and reverse sweep (*y*-axis) are plotted as a function of the first sweeps (*x*-axis) for MP (bottom left) and QP (bottom right) configurations. *R* values are based on Pearson's correlation analysis and were significant with a $p < .001$.

difference between the two runs (averaged across electrode number, stimulation mode, and subject), which was 1.68 dB for the adaptive forced-choice procedure and 2.64 dB for the sweep procedure. Thus the test–retest reliability of the traditional method is better than that of the new sweep method, although the difference in rms error is less than 1 dB. There is no clear interpretation of the three-way interaction term and, given its small effect size and marginal significance, it is unlikely to be of importance.

Testing Time

A primary goal of this research was to test whether the threshold procedure can be performed within a timeframe that makes it clinically feasible. The duration of testing time was substantially shorter for the channel sweep procedure than for the adaptive forced-choice procedure. The total testing time, in minutes, to complete the first two runs for the traditional (open) and sweep (filled) procedures is shown in Figure 8. The average time to complete two runs per electrode for the adaptive procedure was 40.8 min for the MP mode and 49.5 min for the QP mode, while the time to complete two runs (two upward and two downward sweeps) for the channel sweep procedure was 11.4 and 12.1 minutes for the MP and QP stimulation modes, respectively. This is an improvement in testing speed by approximately a factor of 4. This factor would be expected to be similar if only one run of each were performed; in that case, the time for the sweep method could be reduced to around 6 min. A repeated-measures ANOVA was performed with the log-transformed completion time as the dependent variable and procedure and stimulation mode as factors. As expected, there was a significant main effect of procedure ($F(1, 15) = 779$, $p < .001$, partial $\eta^2 = .981$). The main effect of stimulation mode was also significant ($F(1, 15) = 15.0$, $p = .001$, partial $\eta^2 = .501$), as was the interaction between factors ($F(1, 15) = 5.73$, $p = .03$, partial $\eta^2 = .276$).

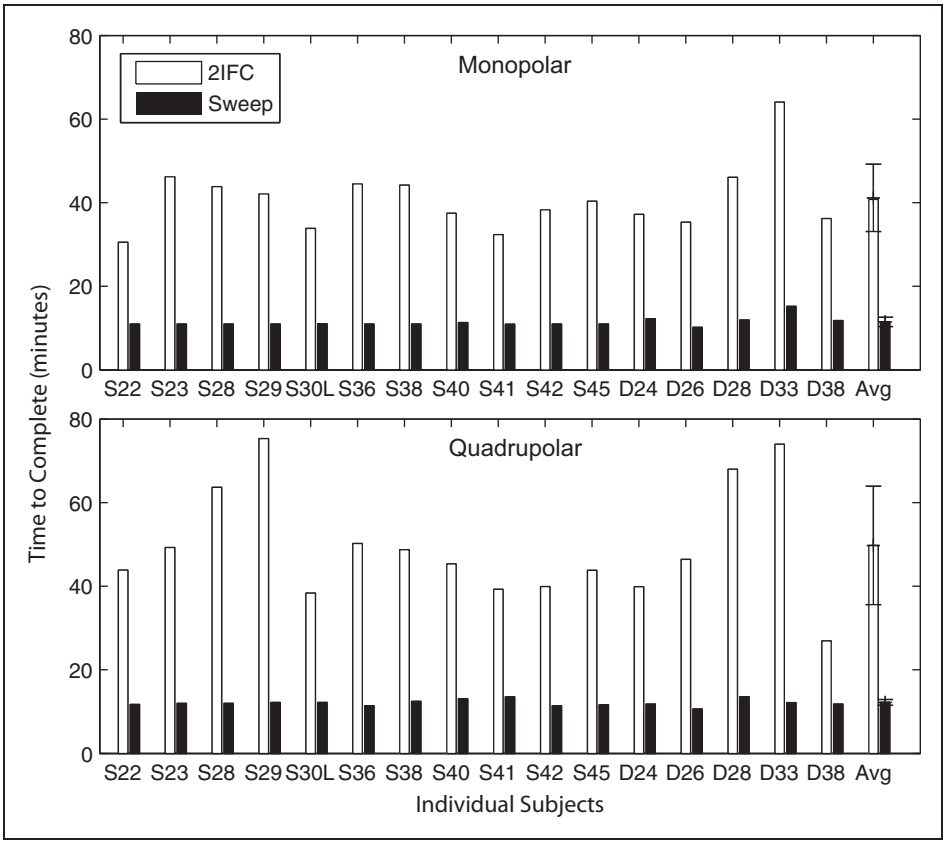

Figure 8. Duration of testing for sweep (open) and 2IFC (filled) methods. Each pair of bars represent data for one subject and data averaged across subjects is the rightmost pair of each panel. Error bars represent the standard deviation. The height of the bar indicates the time it took (in minutes) to complete threshold estimates for each subject using the sweep and 2IFC procedures. Data are shown for MP (top) and QP (bottom).

Comparison of Different Focused Stimulation Methods

Previous research on focused stimulation conducted at the University of Washington laboratory was based on the more common pTP electrode configuration. We compared thresholds obtained with the QP configuration with those using the pTP configuration for the nine subjects tested at the University of Washington. The pTP mode consists of a single active electrode and two flanking electrodes that share the return current. A fraction of 10% of the return current was delivered to the extracochlear ground electrode, corresponding to pTP stimulation with a sigma of .9. Traditional thresholds were compared between pTP and the two nonsteered QP configurations corresponding to the same active electrode with alpha at 0 and 1. For example, if Electrode site 4 serves as the active electrode for the pTP configuration, that same site would also be the active electrode for both the QP 3/4 electrode pair (with $\alpha = 1$) and the 4/5 electrode pair (with $\alpha = 0$). For this analysis, only three active electrodes were tested in each subject (4, 9, and 13) and the data are shown in Figure 9. The thresholds were highly significantly correlated among the pTP and two QP electrode configurations. This suggests that the QP sweep thresholds, which were measured using a constantly changing steered configuration, are effectively equivalent to those obtained with a static nonsteered configuration. Moreover, the absolute similarity of the thresholds suggests that the focusing capabilities of the two configurations are comparable.

Discussion

Consistent with previous studies, psychophysical thresholds are variable across CI subjects and within subjects from electrode to electrode. The variability is particularly large when focused electrical fields are used, such as those obtained with QP stimulation (e.g., Bierer, 2007; Pfingst et al., 2004). As a check, thresholds with QP were found to be nearly identical to those obtained with the more widely tested pTP configuration (e.g., Bierer & Faulkner, 2010; Bierer & Nye, 2014).

Inspired by procedures devised for the acoustic domain (e.g., Sek & Moore, 2011), we developed and tested a method to obtain thresholds in CI listeners by sweeping the centroid of electrical stimulation across the

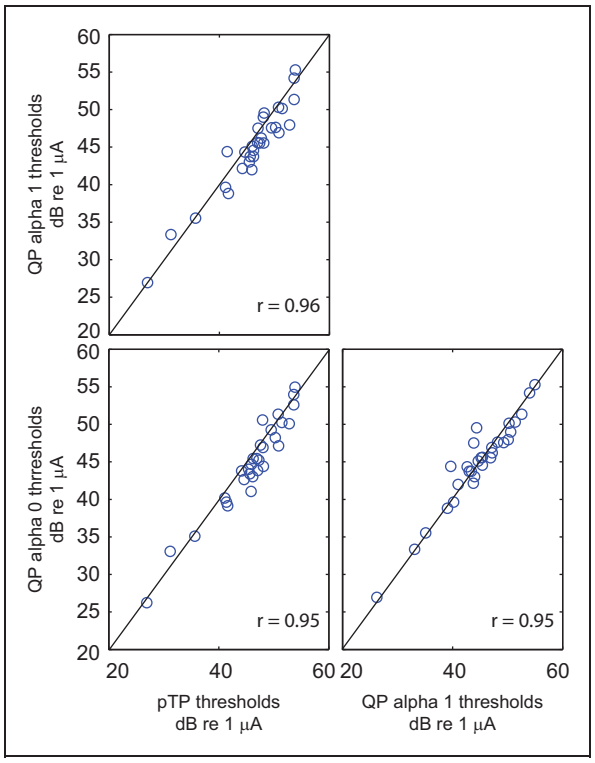

Figure 9. Comparison of threshold estimates using the 2IFC procedure with steered QP and pTP configurations. Left panels represent pTP thresholds (*x*-axis) versus QP thresholds with an alpha of one (top) and zero (bottom). The lower right panel shows threshold estimates for steered QP with alpha of 1 (*x*-axis) and alpha of zero (*y*-axis). *R* values are based on Pearson's correlation analysis and were significant ($p < .001$).

cochlea while varying current level adaptively. The average thresholds and trial-to-trial variability using the novel sweep method were similar to those obtained with the more conventional adaptive forced-choice procedure, for both focused and broad electrode configurations. Although the electrodes at the end of the array were not significantly different with the two procedures, future versions of the software will require one reversal for the end electrodes before beginning the sweep. The results also showed that the new sweep method is approximately a factor of 4 times faster for the same number of threshold estimates, bringing it within the realm of possibility for clinical use. Thus, this method could be applied clinically in devices that support current steering (i.e., those with multiple independent current sources that can be controlled in software).

Srinivasan et al. (2013) have recently demonstrated improved speech perception in noise when employing focused stimulation. As investigators in this field further explore how best to program implants with focused electrical fields (Berenstein, Mens, Mulder, & Vanpoucke, 2008; Srinivasan et al., 2013), the sweep method could be implemented clinically to assist in the fitting procedure. When programming focused strategies, because the thresholds can be highly variable from channel-to-channel, it may be critical to measure individual channel thresholds. If the channel-to-channel variability is not addressed with the measurement of thresholds, stimulation produced by some sounds will be inaudible while others could be mapped too high in the electrical dynamic range producing a distorted signal. In addition to the potential benefits of focused stimulation discussed thus far, thresholds might be used for diagnostic purposes, specifically for evaluating the electrode–neuron interface (Bierer, 2010; Long et al., 2014). For instance, it has been reported that channels with high thresholds have broader psychophysical tuning curves (Bierer & Faulkner, 2010) and smaller dynamic ranges (Bierer & Nye, 2014) than channels with low thresholds. The methodology described here provides an efficient way to obtain these important measurements, which could ultimately lead to improvements in fitting strategies.

Declaration of Conflicting Interests

The authors declared no potential conflicts of interest with respect to the research, authorship, and/or publication of this article.

Funding

The authors disclosed receipt of the following financial support for the research, authorship, and/or publication of this article: This work was supported by NIDCD grants R01 DC012142 (J. A. B.) and R01 DC012262 (A. J. O.).

Acknowledgments

The authors thank the CI subjects who ever so patiently participated in this study. The authors also thank Emily Ellis, AuD, for her assistance with subject recruitment, data collection, and figure preparation, and Leonid Litvak and Kanthiah Koka from Advanced Bionics for technical support. For those interested in obtaining the software used in this study, please go to https://sites.google.com/site/biererlab/bierer-lab-resources.

References

Berenstein, C. K., Mens, L. H., Mulder, J. J., & Vanpoucke, F. J. (2008). Current steering and current focusing in cochlear implants: comparison of monopolar, tripolar and virtual channel electrode configurations. *Ear and Hearing*, *29*, 250–260.

Bierer, J. A. (2007). Threshold and channel interaction in cochlear implant users: Evaluation of the tripolar electrode configuration. *Journal of the Acoustical Society of America*, *121*, 1642–1653.

Bierer, J. A. (2010). Probing the electrode-neuron interface with focused cochlear implant stimulation. *Trends in Amplification*, *14*, 84–95.

Bierer, J. A., & Faulkner, K. F. (2010). Identifying cochlear implant channels with poor electrode–neuron interface:

Partial tripolar, single-channel thresholds, and psychophysical tuning curves. *Ear and Hearing*, *31*, 247–258.

Bierer, J. A., & Middlebrooks, J. C. (2002). Auditory cortical images of cochlear-implant stimuli: Dependence on electrode configuration. *Journal of Neurophysiology*, *87*, 478–492.

Bierer, J. A., & Nye, A. D. (2014). Comparisons between detection threshold and loudness perception for individual cochlear implant channels. *Ear and Hearing*, *35*, 641–651.

Friesen, L. M., Shannon, R. V., Baskent, D., & Wang, X. (2001). Speech recognition in noise as a function of the number of spectral channels: Comparison of acoustic hearing and cochlear implants. *Journal of the Acoustical Society of America*, *110*, 1150–1163.

Jolly, C. N., Spelman, F. A., & Clopton, B. M. (1996). Quadrupolar stimulation for cochlear prostheses: Modeling and experimental data. *IEEE Transactions on Biomedical Engineering*, *43*, 857–865.

Kral, A., Hartmann, R., Mortazavi, D., & Klinke, R. (1998). Spatial resolution of cochlear implants: The electrical field and excitation of auditory afferents. *Hearing Research*, *121*, 11–28.

Landsberger, D. M., Padilla, M., & Srinivasan, A. G. (2012). Reducing current spread using current focusing in cochlear implant users. *Hearing Research*, *284*, 16–24.

Litvak, L. M., Spahr, A. J., Saoji, A. A., & Fridman, G. Y. (2007). Relationship between perception of spectral ripple and speech recognition in cochlear implant and vocoded listeners. *Journal of the Acoustical Society of America*, *122*, 982–991.

Levitt, H. (1971). Transformed up-down methods in psychoacoustics. *Journal of the Acoustical Society of America*, *49*, 467–477.

Long, C. J., Holden, T. A., McClelland, G. H., Parkinson, W. S., Shelton, C., Kelsall, D. C., . . . ,Smith, Z. M. (2014). Examining the electro-neural interface of cochlear implant users using psychophysics, CT scans, and speech understanding. *Journal of the Association in Research in Otolaryngology*, *15*, 293–304.

Nelson, D. A., Donaldson, G. S., & Kreft, H. (2008). Forwardmasked spatial tuning curves in cochlear implant users. *Journal of the Acoustical Society of America*, *123*, 1522–1543.

Oxenham, A. J., & Kreft, H. A. (2014). Speech perception in tones and noise via cochlear implants reveals influence of spectral resolution on temporal processing. *Trends in Hearing*, *18*, 1–14.

Pfingst, B. E., Franck, K. H., Xu, L., Bauer, E. M., & Zwolan, T. A. (2001). Effects of electrode configuration and place of stimulation on speech perception with cochlear prostheses. *Journal of the Association in Research in Otolaryngology*, *2*, 87–103.

Pfingst, B. E., Xu, L., & Thompson, C. S. (2004). Across-site threshold variation in cochlear implants: Relation to speech recognition. *Audiology & Neurotology*, *9*, 341–352.

Rodenhiser, K. L., & Spelman, F. A. (1995). A method for determining the driving currents for focused stimulation in the cochlea. *IEEE Transactions on Biomedical Engineering*, *42*, 337–342.

Sek, A., Alcantara, J., Moore, B. C., Kluk, K., & Wicher, A. (2005). Development of a fast method for determining psychophysical tuning curves. *International Journal of Audiology*, *44*, 408–420.

Sek, A., & Moore, B. C. (2011). Implementation of a fast method for measuring psychophysical tuning curves. *International Journal of Audiology*, *50*, 237–242.

Snyder, R. L., Bierer, J. A., & Middlebrooks, J. C. (2004). Topographic spread of inferior colliculus activation in response to acoustic and intracochlear electric stimulation. *Journal of the Association for Research in Otolaryngology*, *5*, 305–322.

Srinivasan, A. G., Padilla, M., Shannon, R. V., & Landsberger, D. M. (2013). Improving speech perception in noise with current focusing in cochlear implant users. *Hearing Research*, *229*, 29–36.

Teymouri, J., Hullar, T. E., Holden, T. A., & Chole, R. A. (2011). Verification of computed tomographic estimates of cochlear implant array position: A micro-CT and histological analysis. *Otology and Neurotology*, *32*, 980–986.

von Wallenberg, E. L., Battmer, R. D., Doden, I., Gnadeberg, D., Hautle, K.Lenarz, T. (1995). Place-pitch and speech perception measures with bipolar and monopolar electrical stimulation of the cochlea. *Annals of Otology, Rhinology, and Laryngology*, *166*, 372–375.

Zwicker, E. (1974). On the psychophysical equivalent of tuning curves. In E. Zwicker, & P. Terhardt (Eds.), *Facts and models in hearing* (pp. 132–141). Berlin: Springer-Verlag.

Zwolan, T. A., Kileny, P. R., Ashbaugh, C., & Telian, S. A. (1996). Patient performance with the Cochlear Corporation "20 + 2" implant: Bipolar versus monopolar activation. *American Journal of Otology*, *17*, 717–723.